Band gap gratings using quantum well intermixing for quasi-phase-matching

A. S. Helmy,[a] A. C. Bryce,[b] D. C. Hutchings,[b] J. S. Aitchison, and J. H. Marsh[c]
Edward S. Rogers Sr. Department of Electrical and Computer Engineering, University of Toronto, 10 King's College Road, Toronto, Ontario M5S 3G4, Canada

(Received 4 July 2006; accepted 9 October 2006; published online 27 December 2006)

In this work, the spatial resolution of two quantum well intermixing processes has been obtained using spatially resolved photoluminescence. The processes investigated are impurity-free vacancy disordering using SiO_2/SiO_2:P caps and sputtered silica induced intermixing. These studies aimed to choose a suitable intermixing technology to realize the band gap gratings for domain disordering quasi-phase-matching in GaAs/AlGaAs heterostructures. From the photoluminescence studies it was established that the process of impurity-free vacancy disordering using SiO_2/SiO_2:P caps has a spatial resolution on the order of 7 μm, while the process of sputtered silica induced intermixing has a spatial resolution on the order of 3 μm. From these measurements it was demonstrated that the sputtered silica induced intermixing process is more suitable for the fabrication of the gratings needed for quasi-phase-matching in the samples studied here. Successful quasi-phase-matching demonstrated through second harmonic generation at 775 nm has been produced in GaAs/AlAs short superlattice waveguides using sputtered silica induced intermixing through domain disordering quasi-phase-matching. The gratings have shown a duty cycle far from the targeted 1:1 design, which has implications on the conversion efficiency. © *2006 American Institute of Physics*.
[DOI: 10.1063/1.2402034]

I. INTRODUCTION

Postgrowth lateral band gap engineering of quantum confined heterostructures using quantum well intermixing (QWI) has reached sufficient maturity to allow its utilization beyond monolithic photonic device integration. QWI can also be used for providing enhanced functionality for III-V photonics. This is obtained through the control they provide over the linear and nonlinear optical properties over scales on the order of one wavelength.[1] The use of second order nonlinearities in III-V semiconductors, for example, offers the possibility of efficient optical frequency conversion, monolithically integrated parametric oscillators, correlated photon pair sources, and cascaded Kerr-like nonlinearities, only to name a few. Particularly in III-V quantum confined heterostructures, where large $\chi^{(2)}$ coefficients can be obtained,[2] a multitude of efficient functional devices, ranging from integrated second harmonic generation structures to integrated devices for parametric generation, oscillation, and amplification, could be realized.[3,4] The challenge in using III-V semiconductors is to achieve phase matching between the interacting waves. QWI technology has demonstrated the ability to modulate the resonant part of the second order nonlinear optical coefficients in GaAs/AlAs superlattice structures, which leads to successful quasi-phase-matching and second harmonic generation (SHG) in waveguide structures with a GaAs/AlAs superlattice core.[1] As the functionality provided by QWI technologies for applications grows more mature, the need arises to optimize these processes to suit each application. It is also necessary to determine the limitations of each technique in order to use the most suited one for each application. Hence it is essential to comprehensively characterize and control numerous attributes of the various QWI technologies available.

Some examples of QWI attributes that are important to many applications are the change in the refractive index, its dispersion, and the reduction in the birefringence resulting from the obtained band gap shifts. These parameters play a pivotal role in determining the conversion efficiency in quasi-phase-matched (QPM) structures for frequency conversion applications in GaAs/AlGaAs heterostructures.[5] Another parameter of interest is the control of the spatial selectivity of QWI technologies in practical *p-i-n* structures, which is a key for numerous applications where active and passive devices are integrated. The integration of various photonic devices relies heavily on the quality and extent of the interface between regions of different band gaps as they always constitute the divide between active and passive sections. More specific to this work, the spatial resolution, magnitude of band gap modulation, and interface quality of a given QWI technology are all of paramount importance to the QPM conversion efficiency if this technology is to be used to obtain domain disordering. As such, this work will study the spatial resolution of two fabrication processes available for realizing the band gap gratings used in QPM structures.

The QWI technology of choice in this work is impurity-free vacancy disordering (IFVD). It is a popular QWI technique due to its simplicity and suitability for batch process-

[a]Electronic mail: a.helmy@utoronto.ca
[b]Also at Electronics and Electricals Engineering, University of Glasgow, Glasgow G12 8QQ, UK.
[c]Also at Intense, Hamilton International Technology Park, Glasgow, G72 0BN, UK.

ing in the photonics industry.[6] This technique is based on rapid thermal processing of the quantum confined heterostructures in the presence of dielectric caps on the surface of the epilayer. These caps promote or inhibit intermixing depending on the stress they exert on the wafer surface and on the solubility of the epilayer lattice constituents within them due to the stress fields. It is the lattice constituent outdiffusion that generates the vacancies which cause interdiffusion.[7,8] The majority of the studies carried out to date on the spatial selection of IFVD involved characterizing either the interface between two large areas of intermixed and intermixing-suppressed regions, or features with widths less than 100 nm at a depth less than 100 nm from the surface for one dimensional (1D) and zero dimensional (0D) confinement.[7,9] Features that lie in the range of 1–10 μm in practical *p-i-n* laser structures are of interest because they can be used to integrate various devices such as waveguides[10] and domain disordering for QPM in quantum confined heterostructures with semiconductor diode lasers.[1] To date, little work has been reported on features in this regime using IFVD in practical *p-i-n* structures where lasers, modulator waveguides, and amplifiers can be integrated with other functional devices, and more importantly where the quantum wells lay in excess of 1 μm from the surface. The depth of the quantum confined heterostructures is an issue that is often overlooked when assessing a given QWI technology and its spatial resolution, since the QWI is highly dependent on depth.[8] Therefore there is an eminent need to establish the resolution limit of IFVD in practical structures.

In order to better understand the capability of the technologies studied here in defining small features in the band gap, we choose to study isolated features in the range of dimensions of interest rather than 1:1 gratings. After establishing the technology of choice, 1:1 gratings are then fabricated, and nonlinear optical QPM experiments conducted. In this work spatially resolved photoluminescence (PL) measurements, with a 1 μm step and a spot size of $\sim$0.5 μm, were carried out at room temperature.[11] In contrast, previous measurements of periodic structures produced by QWI were carried out with periods of $>$20 μm, and varying duty cycles of intermixed to intermixing-suppressed features were investigated.[12] Large-area optical excitation was carried out in those studies. The PL resolution limit was established in this work when the peaks from the intermixed and intermixing-suppressed regions merge. Spatially and spectrally resolved measurements of features, in the size regime of 1–10 μm, fabricated using IFVD have not been carried out previously and can provide tremendous insight into the capabilities and mechanisms of this technology.

II. STUDYING THE RESOLUTION OF TWO QWI TECHNIQUES

Two IFVD technologies have been examined in this work with the aim of choosing the most suitable for fabricating the band gap gratings required for the QPM samples. The first technology is the IFVD using SiO_2 and SiO_2:P dielectric caps,[6] while the second is intermixing using sputtered SiO_2 induced defects, a technique which combines the use of IFVD with defects introduced during sputtering to induce intermixing.[13]

SiO_2 has long been known as an effective intermixing promoter in the GaAs/AlGaAs system. Conversely SiO_2:P was previously found to have good performance in inhibiting QWI, which was attributed to the effect of phosphorus on the SiO_2 films.[6] The addition of phosphorus into the SiO_2 film leads to an increase in the thermal expansion coefficient[14] and a decrease in the glass softening temperature,[15] which result in a reduction of the thermal stress in the film. Therefore, less compressive strain will be induced in the GaAs surface layer during the annealing step, and as a result, the number of Ga vacancies will be reduced due to less Ga outdiffusion.[6]

The epitaxial structure of the samples was that of a *p-i-n* doped laser structure with two 10 nm GaAs quantum wells in $Al_{0.2}Ga_{0.8}As$ barriers. The QWs were at a depth of 1 μm below the surface.[6] Photoresist stripes with widths varying from 2 to 20 μm, with a 35 μm separation, were covered with 200 nm of SiO_2:P using photolithography and wet etching, while the rest of the sample was covered with electron gun (e-gun) evaporated SiO_2. The P doping was 5% in weight and was incorporated in the SiO_2 using a separate PH_3 flow line during plasma enhanced chemical vapor deposition (PECVD), while the e-gun deposition used a SiO_2 target to deposit a 200 nm layer on the samples. The sample would then produce intermixing-suppressed features between 2 and 20 μm after annealing at 925 °C for 60 s with a rise time of 15 s. The sputtered SiO_2 layer was 200 nm thick and was deposited on the sample using a SiO_2 sputtering target. The sputtered SiO_2 layer was first patterned with the same photoresist stripes as described for the first sample, then the sputtered SiO_2 was deposited on the surface, after which lift-off was carried out. A 200 nm thick layer of e-gun SiO_2 was then deposited. Samples were annealed for 60 s at 725 °C with a rise time of 15 s. The sample would then produce intermixing-suppressed features between 2 and 20 μm.

The PL measurements were carried out using a *Jobin Yvon Horriba* high resolution Raman scope equipped with a sample positioning stage which has a precision *XY* mechanical system with a 0.1 μm resolution. However, the spatial resolution is still limited by the laser beam spot size, which is 0.5 μm, and hence the step size was kept at 1 μm. The laser used for probing was an Ar^+ 514 nm laser. A software was used to define and undertake the area scan; it was also used to carry out the curve fitting of the data after. The properties of the curve fitted graphs are then plotted as a function of position on the sample.

The differential wavelength shift between the intermixed and as grown PL peaks, plotted as a function of length along the features, can be seen in Figs. 1 and 2 for the samples fabricated using SiO_2/SiO_2:P and sputtered SiO_2, respectively. For the larger intermixing-suppressed stripe sizes between 8 and 20 μm for the SiO_2/SiO_2:P sample, the differential PL shift underneath the SiO_2:P is independent of the feature size and is equal to 40 nm. However, for the smaller stripes, i.e., stripes $<$8 μm, the differential PL shift depends

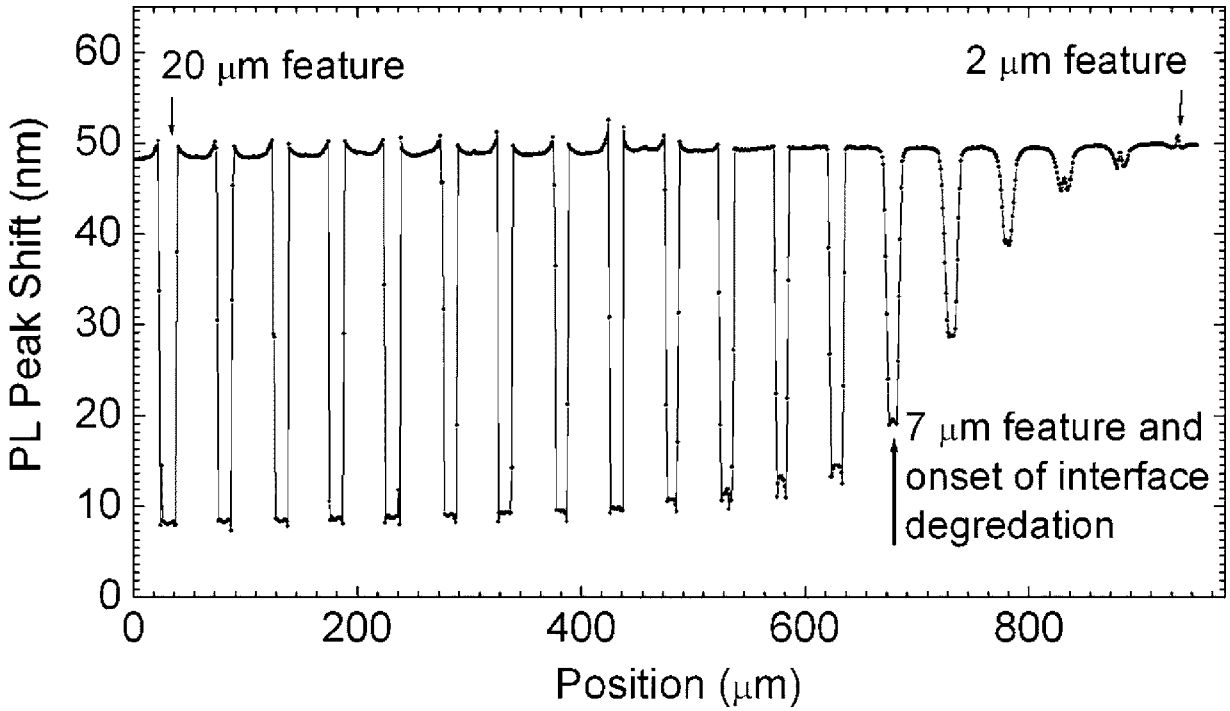

FIG. 1. The multiple quantum well (MQW) PL peak position shift as a function of position along features (stripes) with sizes varying between 2 and 20 μm stripes and incrementing with 1 μm step. The stripes are all separated by a 35 μm gap. The samples were intermixed using IFVD process with SiO_2/SiO_2:P caps. The PL shift is calculated with respect to the as grown sample wavelength. The step size of the *XY* stage used in the PL measurements is 1 μm.

on the feature size, decreasing as the feature size is reduced. As for the sputtered SiO_2 sample, larger stripe sizes between 4 and 20 μm exhibit nearly uniform differential PL shift under the e-gun SiO_2, equal to 30 nm. The differential PL shift for smaller cap sizes, i.e., stripes <4 μm, also depends on the feature size as in the first case studied, decreasing as the feature size is reduced. It should be noted nonetheless that for the case of sputtered silica process, as can be seen in Fig.

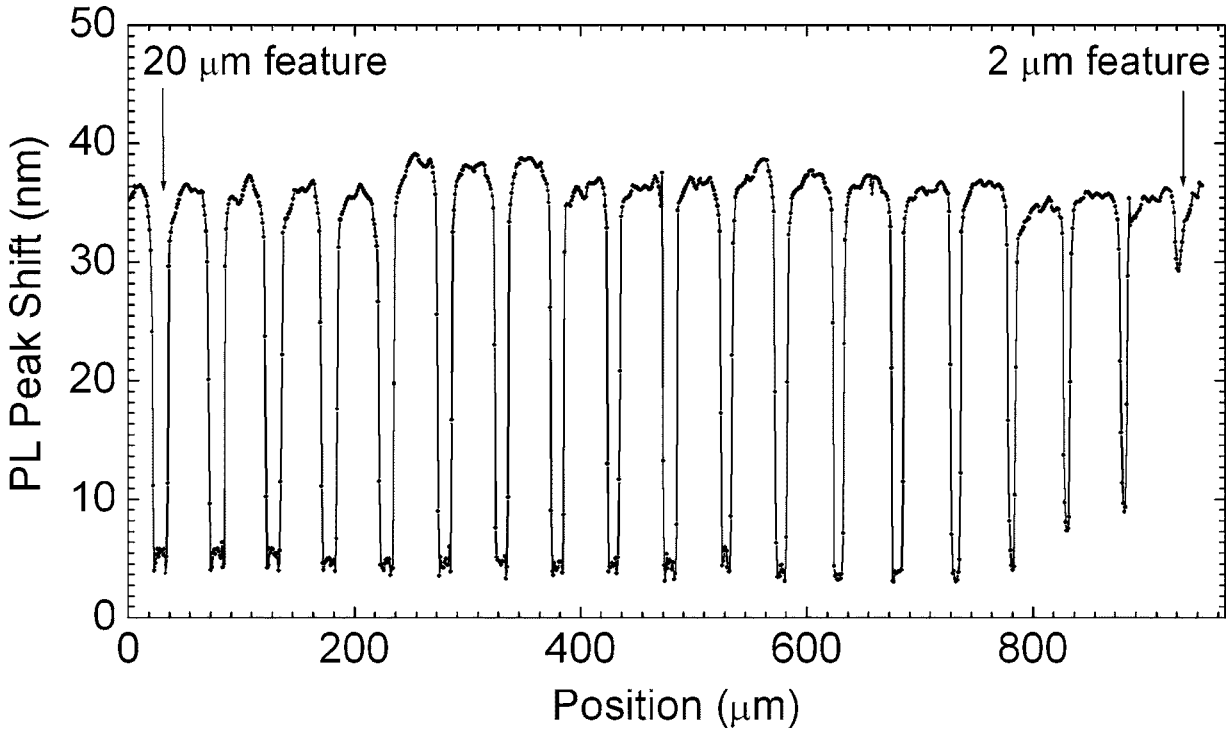

FIG. 2. The MQW PL peak position shift as a function of position along features (stripes) with sizes varying between 2 and 20 μm stripes incrementing with 1 μm step. The stripes are all separated by a 35 μm gap. The samples were intermixed using sputtered silica induced intermixing. The PL shift is calculated with respect to the as grown sample wavelength. The step size of the *XY* stage used in the PL measurements is 1 μm.

2, a finite differential band gap shift equal to 7 nm between the areas underneath the e-gun and the sputtered silica can still be attained for the 2 μm feature.

The resolution limit for the sputtered silica samples can be readily explained if the extent of the lateral defect diffusion from the areas covered with sputtered silica into those covered by e-gun silica is taken into account. The transition between the intermixed and intermixing-suppressed regions in all the features is on the order of two to three data points which correspond to an interface region of 2–3 μm. As the sizes of the intermixing-suppressed regions approach a value of 2–3 μm, the effectiveness of the intermixing suppression is reduced due to the presence of excess defects laterally diffusing from the sputtered silica regions. Consistent with this picture, the intermixing suppression is compromised starting from features of 5 μm as can be seen from Fig. 2 and it monotonically deteriorates as the feature size is reduced.

The behavior observed in the samples with SiO_2/SiO_2:P caps is more intricate. For features >7 μm the amount of intermixing suppression is independent of the feature size. Moreover the transition region between the intermixing enhanced and intermixing-suppressed areas takes place within one to two data points which translate to 1–2 μm. For feature sizes smaller than 7 μm, not only does the intermixing-suppression performance degrade but also the transition region between the intermixed and intermixing-suppressed regions increases, spanning more than four data points. The grading in the band gap is a physical effect rather than an artifact of the photogenerated carrier diffusion length. This is because the measurement system could detect shorter transition periods as seen for larger feature sizes. It is also interesting to note that for the 2 μm stripe, the band gap shift underneath the SiO_2:P is effectively identical to that observed under the SiO_2 areas between the stripes; hence no intermixing suppression could be achieved for the 2 μm stripe. The observed size dependence of intermixing suppression, if considered by itself, can be ascribed due to the finite diffusion length. However, the feature size where both behaviors take place, the size dependence on intermixing as well as the increased extent of interface region, is identical and is 7 μm for these samples, as indicated in Fig. 1. This strongly suggests that the film stress plays a pivotal role in the QWI process of IFVD using SiO_2/SiO_2:P caps. Dielectric film stress has been long suspected as a chief mechanism for IFVD. Recent measurements, which were carried out on isolated SiO_2/SiO_2:P features as well as 1:1 SiO_2/SiO_2:P gratings, corroborate the theory that the film stress as well as the stress originating from the film edge play pivotal roles in defining the behavior of a given film structure in the IFVD process using SiO_2/SiO_2:P caps.[16,17]

Before we can draw conclusions about the capabilities of both technologies it is important to bear in mind that the processes involved in both fabrication technologies are quite different. The wet etching associated with the SiO_2/SiO_2:P process involves graded etching profiles which may influence the QWI behavior. As will be discussed later in this work QWI in IFVD is highly dependent on the stress field generated at the dielectric/substrate interface. The lift-off step in case of the sputtered silica process may also cause nonideal undercut profile of the dielectric caps, which will in turn influence the QWI behavior of the process. In addition, residual photoresist can potentially result from this process and may explain the varying behavior between both intermixing profiles. Therefore it is likely that variation in the shapes and profiles of the dielectric caps in both processes will have influence on the QWI performance due to the substantial modification they can inflict on the stress fields at the interface of the dielectric caps.

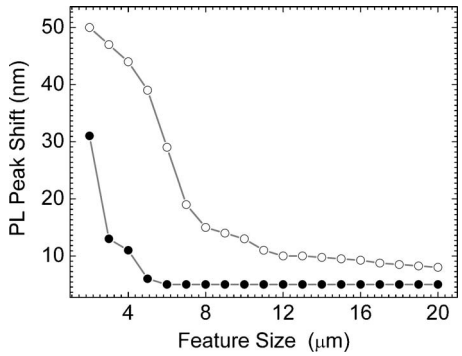

FIG. 3. A comparison of the PL shift between the intermixing-suppressed regions for the samples intermixed using both techniques. The superior spatial resolution of the sputtered silica process is evident.

In Fig. 3, the wavelength shift between the intermixed and intermixing-suppressed regions is plotted as a function of stripe width for both samples, as this differential shift is considered the useful parameter for practical applications as opposed to the absolute shift of both regions with respect to the as grown wafer. It is clear that the sputtered SiO_2 process has superior spatial resolution compared with that of SiO_2/SiO_2:P IFVD, as demonstrated by the measurements. The spatial resolution of the sputtered silica process seems, from this comparison, to suffice for use in fabricating QPM gratings which have intermixing-suppressed regions $>2-3$ μm which translate to periods >5 μm. Before moving on to fabricate the QPM gratings using the sputtered silica process it is imporant to note that we have gone further to investigate more closely the spatial resolution of the SiO_2/SiO_2:P IFVD process to observe some interesting effects in 1:1 gratings with periods between 1 and 10 μm. The results confirmed that it was not possible to use the process we desribed to realize band gap gratings with dimensions of $<4-5$ μm. More interestingly we have observed that there are effects specific to 1:1 gratings in this dimension regime such as improved inhibition of QWI, which we attributed to lateral stress from the dielectric cap interfaces.[16,17] These initial measurements suggest that while the evidence for the role of stress on vacancy formation has been reported previously, the effects of stress on vacancy migration have not yet been considered and play a major role in the results we observe here. An understanding of both processes is necessary to explain the dependence in the results on the cap sizes. The presence of stress fields affects both the diffusive and drift components of vacancy flux, as well as their equilibrium concentration. A nonuniform stress field, where the gradient is nonzero, acts as a driving force for vacancies, causing

them to drift from areas that are less compressive (more tensile) to areas that are more compressive (less tensile). In addition, compressive stress acts to decrease the diffusion coefficient, while the opposite is true for tensile stress. In dielectric features such as silica on top of GaAs, the tensile stress is usually associated with the edges of the films, while the compressive stress is usually present underneath the area covered by film. The interplay between these effects in films with different dimensions is thought to be the reason behind the strong size dependence on intermixing seen for the SiO2/SiO2:P samples, resulting in no apparent differential shift for 2 μm features.

With careful inspection of the spatially resolved PL of both samples shown in Figs. 1 and 2, one can identify the difference in the shape of intermixing exhibited by each process. While the features realized using SiO_2/SiO_2:P caps have a flattop profile and a grading at the feature edges, those realized using sputtered silica have a grading in the band gap with the maximum intermixing realized at the center of the film. This can be understood when the details of each process are studied.

- The annealing in the SiO_2/SiO_2:P cap process takes place at temperatures $>900\,^{\circ}C$, where the thermal mismatch between the dielectric and the substrate is substantial.[7,9,14,17] The vacancy defect generation on the interface and their subsequent diffusion towards the QWs is the most dominant promoter of intermixing. The defect generation will take place within the area covered by the intermixing promoter cap, namely, the SiO_2 cap, where the stress takes place. It will therefore be reduced closer to the interface between the SiO_2 and SiO_2:P.[17]
- The annealing temperature in the sputtered silica process takes place usually at temperatures $\sim 800\,^{\circ}C$. At these temperatures the role of the defect diffusion due to stress formation at the interface is less dominant. Equally important is the role played by the deposition process which involves ions generated in the plasma that will also contribute to the QWI process. The graded profile of the intermixing is thought to be generated due to the complex interplay between these two mechanisms.[13]
- Another source of the discrepancy can be the finite error in the curve fitting routine. Each of the two figures (Figs. 1 and 2) are made of ~ 1000 spectra which are curve fitted using a regression routine. The curve fitting takes place against a background signal and noise from the detector which reduces the signal to noise ratio for fitting. The interface regions, particularly where two peaks may be present on the graph, are likely to suffer the most from these curve fitting uncertainties and may produce some inconsistencies in the PL peak wavelength.[17]
- The fabrication process used in both processes may introduce its own intricacies to the intermixing process. For example, excess resist that was not removed during the sputtered silica process may exhibit unpredictable effects. Moreover, the under- or overcutting involved in lift-off and wet etching is likely to produce different stress fields at the interface between different dielectric caps. This will also contribute to defect diffusion and drift components which may govern the QWI intermixing process on the edges.[13,17,18]

III. FABRICATION OF BAND GAP GRATINGS FOR QPM EXPERIMENTS

The structure used for the QPM experiments comprises of 0.6 μm of a symmetric superlattice (SL) waveguide core made of 14:14 monolayers of GaAs:AlAs, respectively. The lower and upper claddings were bulk $Al_{0.6}Ga_{0.4}As$ of 1.5 and 1 μm widths, respectively. A 100 nm GaAs cap was used to cover the upper cladding. The structure was nominally undoped grown by molecular beam epitaxy (MBE) on a semi-insulating GaAs substrate. The room temperature PL emission wavelength of the structure was 745 nm from the central portion of the wafer. This design allows us to assess QPM using the SHG experiment with the operating fundamental wavelength, ~ 1550 nm, at 30 meV below the half band gap to avoid two-photon absorption and use the modulation attained in the resonant component of $\chi^{(2)}$ as the band gap of the structure is modulated.[1,19] Domain disordering was carried out using the sputtered silica process for a range of grating periods varying between 5 and 12 μm. The samples were processed as per the parameters discussed in the previous sections. Single mode ridge waveguides with widths of 2 μm were defined on the sample orthogonal to the gratings using plasma etching. The setup used to test the samples has been described previously and is based on a synchronously pumped, singly resonant femtosecond periodically poled lithium niobate (PPLN) optical parametric oscillator based on a semi-monolithic cavity design. Successful type-I phase matching has been confirmed through second harmonic generation that is transverse magnetic (TM) polarized at 775 nm with a transverse electric (TE) polarized pump at 1550 nm.[1,20] Spatially resolved PL has been then carried out across several periods of various gratings within the sample. Due to the finite thickness of the superlattice in comparison to the double quantum well samples used to compare the QWI technologies in the previous section, incomplete intermixing along the layer depth is likely. Therefore when investigating these structures a careful study of the collected spectra must be taken into account. After annealing, the room temperature PL wavelength was measured using the spatially resolved PL setup described above; however, the spectra were collected with a step of 0.5 μm. In addition, a sample is cleaved off the wafer, and the grating is probed edge-on from the cleaved facet instead of probing from the top surface of the wafer. This facilitates observing incomplete intermixing along the depth of the 600 nm thickness of the superlattice layer. The line scan position is shown superimposed on a schematic of the sample in Fig. 4. The spectra as a function of the position on the wafer are plotted in Fig. 5 for four periods of a 10 μm grating. Various interesting features can be extracted from the figure.

- The duty cycle of the grating which was defined as 1:1 vastly deviates from this figure and it is close to 30:70.

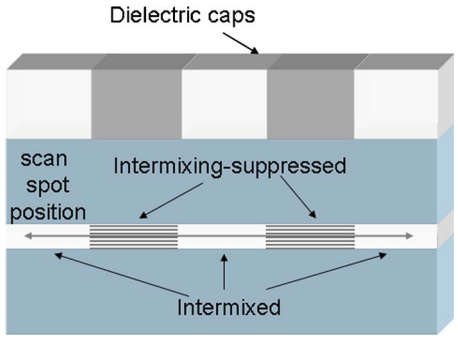

FIG. 4. (Color online) A schematic diagram of the QPM sample and the position of the laser spot while taking the line scan across the cross section of the sample coinciding with the SL core.

Although this does not have an impact on the phase matching wavelength, it may have an impact on the conversion efficiency. An optimization in the mask dimensions can be used to counteract the defect diffusion effects which may cause this deviation from the mask duty cycle. Other QWI techniques, such as ion implantation induced intermixing can also be used to ensure uniform defect profile across the SL layer.

- The transition between both the intermixed and intermixing-suppressed regions takes place within one to two spectra, which translate to 0.5–1 μm. This value is on the order of both the step size as well as the spot size, which suggests, when taking photogenerated carrier diffusion into account, that the resolution observed is likely to be better than 1 μm. More exact figures need substantially enhanced complexity in the measurements in order to either eliminate the effect of the photogenerated carrier diffusion or to take it into account through deconvolving its contribution to the feature size.[21]
- Complete intermixing is likely to would have taken place throughout the superlattice structure height. This is due to the single peaked spectrum observed in both the intermixed and intermixing-suppressed regions. Incomplete intermixing may have implications on the conversion efficiency. The spot size used is 0.5 μm which covers over 80% of the superlattice layer which has a thickness of 600 nm. This arrangement provides a higher confidence level that the light source excitation reaches the majority of the superlattice layer, hence providing accurate account of the vertical band gap inhomogeneity if existing. Again in this case photogenerated carrier diffusion may arise especially with structures exhibiting two dimensional band gap gradients as the one studied here.[21]
- The grading in the QWI profile, with the edges exhibiting a reduced amount of intermixing compared to the center of the feature which is observed in the isolated features produced using sputtered silica, is also seen in the QPM samples. The effect is much clearer in Fig. 5 than in Fig. 2 due to the enhanced resolution of the measurements conducted on the QPM gratings. As discussed in Sec. II, many effects can contribute to this behavior. Some process-specific effects include residual photoresist and nonrectangular silica profiles due to the lift-off process.[18] In addition some effects due the sputtering deposition mechanisms and its associated defects may influence the intermixing profiles produced.[7,13] The stress induced at the dielectric edges is likely to play a role in affecting the diffusivity and drift of defects, which would in turn result in differences between the amount of defects reaching the SL at the edges of the features in comparison to those at the center. On the other hand this implies that the modulation of intermixing within a feature is likely to be dependent on the feature size, which has not been seen in the sputtered silica process studied here, but has been observed before for IFVD using SiO_2/SiO_2:P caps.[17]

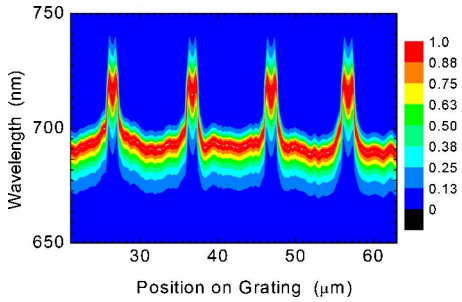

FIG. 5. (Color online) A plot of the PL spectra of a line scan across four periods of a band gap grating fabricated using sputtered silica induced intermixing. The step size of the line scan is 0.5 μm.

IV. DISCUSSION

Knowledge of the attributes of the band gap gratings is key in enabling efficient conversion efficiency using QPM. Properties such as duty cycle, period dimension, interface quality, and refractive index change between the mark and space areas within a period are all important parameters. Initial studies on the IFVD process using spatially and temporally resolved PL were limited by the excitation laser spot size (~2 μm).[22] They were carried out on 1:1 gratings with a period of 16 μm. The measurements reported here are carried out using a confocal system with a superior spatial resolution and a smaller spot size (0.5 μm) and hence are bound to be more accurate. The spatial resolution dependence on the material system, the intermixing process, and the details of heterostructure make it difficult to compare different reports of the resolution of QWI. However, IFVD has shown superior resolution when used on structures within hundreds of nanometer proximity to the surface.[9] During the earlier phase of studying the IFVD process spatial resolution better than 1.5 μm has been reported for QWs at a depth of 500 nm from the surface.[18] In addition the spatial resolution of Ar plasma induced intermixing in the InGaAs/InGaAsP material system has been reported to be on the order of 2.5 μm,[7] while that of pulsed-photoabsorption-induced intermixing in the same material system has been reported to be also on the order of 2.5 μm.[23] Perhaps the highest spatial resolution of active laser structures has been reported using

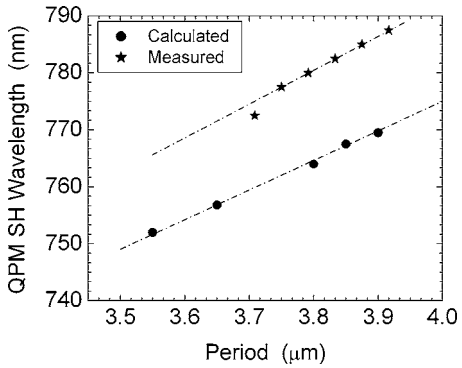

FIG. 6. The measured QPM wavelength versus period compared with the calculated values. The slope of the calculated values, which is in units of nanometer of QPM SH wavelength per micrometer of QPM period, is 52 nm/μm, while that of the measured data is 68 nm/μm.

ion implantation induced intermixing, where resolution on the order of a few hundred nanometers was reported.[24]

We have recently studied the change of refractive index in the intermixed regions in comparison to the as grown SL regions in the waveguide. The measurements provided much insight towards optimizing the QPM grating.[5] However, the study reported here has been essential in determining both the appropriate QWI technology required for the QPM grating fabrication as well as the limitations and attributes of this technology which in turn govern the attainable QPM conversion efficiency. For example, a substantial change in the refractive index between both regions of the grating will result in excessive optical losses and hence reduced conversion efficiency. Similarly a nonideal interface region between the regions will increase the optical scattering losses and result in reduced conversion efficiency. The asymmetric duty cycle observed in this work provides hope that there is ample room for increasing the efficiency when the optimal 1:1 duty cycle is achieved. This work is therefore useful in providing insight into the design and process parameters for fabricating band gap gratings which are optimized to maximize the efficiency of the QPM process in heterostructure semiconductor waveguides. The measurements carried out in this work will also serve as a valuable vehicle to assist further development of the QWI technology of choice. Process parameters such as the annealing conditions, dielectric caps used, and their thickness and deposition conditions can all influence the band gap grating. The spatially resolved PL measurements reported here can therefore be used to optimize these parameters by studying their effects on the quality of the band gap gratings they generate.

In Fig. 6 the calculated periods for type-I phase matching, based on the current slab waveguide measurements, are plotted versus the corresponding QPM SH wavelength. For comparison we also show recent tuning curve results indicating the wavelength for the maximum SH generation for various QPM periods in a strip-loaded waveguide fabricated in a nominally identical wafer. As can been seen from the figure both plots have a similar slope, but the absolute QPM periods obtained for a particular SH peak wavelength in the strip-loaded waveguide are approximately 0.3 μm shorter than that inferred from the current slab waveguide measurements. We attribute this offset to the different guiding structures (two dimensional for the strip loaded versus one dimensional for slab), which will result in a further modification of the effective index, and possible unintentional differences in the MBE growth between the two nominally identical wafers. However, it is reassuring to see that the slope of both tuning curves match as the slopes are dominated by the material dispersion.

V. CONCLUSIONS

The spatial resolution of two quantum well intermixing processes has been studied with the aim of using them in realizing band gap gratings for domain disordering quasi-phase-matching processes in the GaAs/AlGaAs heterostructures. From the measurements discussed above it is clear that the sputtered silica induced intermixing technology is more suitable for the fabrication of the QPM gratings. The spatial resolution processes were studied using spatially resolved PL with a step size of 1 μm. From the PL studies it was established that the process of impurity-free vacancy disordering using SiO_2/SiO_2:P caps has a spatial resolution on the order of 7 μm, while the process of sputtered silica induced intermixing has a spatial resolution better than 3 μm, and hence is suited for fabricating the band gap gratings. Successful QPM through SH generation at 775 nm has been produced in GaAs/AlAs short superlattice waveguides using sputtered silica induced intermixing to achieve domain disordering quasi-phase-matching. The gratings measured have shown a duty cycle far from the targeted 1:1 design, which has implications on the conversion efficiency.

[1] A. S. Helmy, *et al.* Opt. Lett. **25**, 1373 (2000).
[2] J. S. Aitchison, M. W. Street, N. D. Whitbread, D. C. Hutchings, J. H. Marsh, G. T. Kennedy, and W. Sibbett, IEEE J. Sel. Top. Quantum Electron. **4**, 695 (1998).
[3] J. B. Khurgin, E. Rosencher, and Y. J. Ding, J. Opt. Soc. Am. B **15**, 1726 (1998).
[4] *Quantum Well Intermixing for Photonics*, Milestone Series Vol. 145, edited by E. H. Li (SPIE, Washington, DC, 1998).
[5] T. C. Kleckner, A. S. Helmy, K. Zeaiter, D. C. Hutchings, and J. S. Aitchison, IEEE J. Quantum Electron. **42**, 280 (2006).
[6] P. Cusumano, B. S. Ooi, A. S. Helmy, S. G. Ayling, A. C. Bryce, J. H. Marsh, B. Vögele, and M. J. Rose, J. Appl. Phys. **81**, 2445 (1997).
[7] H. S. Djie, T. Mei, and J. Arokiaraj, Appl. Phys. Lett. **85**, 3008 (2004).
[8] P. N. K. Deenapanray and C. Jagadish, J. Vac. Sci. Technol. B **19**, 1962 (2001).
[9] A. Pepin, C. Vieu, M. Schneider, H. Launois, and Y. Nissim, J. Vac. Sci. Technol. B **15**, 142 (1997).
[10] Y. Suzuki, H. Iwamura, and O. Mikami, Appl. Phys. Lett. **56**, 19 (1990).
[11] A. Gustafsson, M. E. Pistol, L. Montelius, and L. Samuelson, J. Appl. Phys. **84**, 1715 (1998).
[12] J. E. Haysom, P. J. Poole, Y. Feng, E. S. Koteles, J. J. He, S. Charbonneau, R. D. Goldberg, and I. V. Mitchell, J. Vac. Sci. Technol. A **16**, 817 (1998).
[13] O. P. Kowalski *et al.*, Appl. Phys. Lett. **72**, 581 (1997).
[14] S. K. Ghandhi, *VLSI Fabrication Principles* (Wiley, New York, 1994), pp. 530–532, and references therein.
[15] T. Y. Tien and F. A. Hummel, J. Am. Ceram. Soc. **45**, 422 (1962).
[16] A. S. Helmy, B. Fung, A. C. Bryce, J. S. Aitchison, and J. H. Marsh, Appl. Phys. Lett. (to be published).
[17] A. S. Helmy, A. C. Bryce, C. N. Ironside, J. S. Aitchison, J. H. Marsh, and S. G. Ayling, Mater. Res. Soc. Symp. Proc. **607**, 509 (2000).
[18] J. Y. Chi, X. Wen, E. S. Koteles, and B. Elman, Appl. Phys. Lett. **55**, 855 (1989).
[19] D. C. Hutchings, Appl. Phys. Lett. **76**, 1362 (2000).
[20] D. C. Hutchings, M. Sorel, K. Zeaiter, A. J. Zilkie, B. Leesti, A. S. Helmy,

P. W. E. Smith, and J. S. Aitchison, *Nonlinear Guided Waves and their Applications, Toronto, Canada* (Optical Society of America,Washington, D.C., 2004), Paper No. TuA5.
[21]A. Gustafsson, M. E. Pistol, L. Montelius, and L. Samuelson, J. Appl. Phys. **84**, 1715 (1998).
[22]A. S. Helmy *et al.*, IEEE J. Sel. Top. Quantum Electron. **4**, 661 (1998).
[23]T. K. Ong, B. S. Ooi, Y. L. Lam, Y. C. Chan, Y. Zhou, and A. S. Helmy, J. Appl. Phys. **87**, 2775 (2000).
[24]J. P. Reithmaier and A. Forchel, IEEE J. Sel. Top. Quantum Electron. **4**, 595 (1998).